Published in final edited form as:
Biochemistry. 2009 June 23; 48(24): 5510–5517. doi:10.1021/bi9006226.

Mechanism of the Orotidine 5'-Monophosphate Decarboxylase-Catalyzed Reaction: Effect of Solvent Viscosity on Kinetic Constants†

B. McKay Wood‡, **Kui K. Chan**‡, **Tina L. Amyes**§, **John P. Richard**§, and **John A. Gerlt**‡,*

‡Departments of Biochemistry and Chemistry, University of Illinois at Urbana-Champaign, Buffalo, NY 14260

§Department of Chemistry, University at Buffalo, Buffalo, NY 14260

Abstract

Orotidine 5'-monophosphate decarboxylase (OMPDC) is an exceptionally proficient catalyst: the rate acceleration (k_{cat}/k_{non}) is 7.1×10^{16} and the proficiency [$(k_{cat}/K_M)/k_{non}$] is 4.8×10^{22} M^{-1}. The structural basis for the large rate acceleration and proficiency is unknown, although the mechanism has been established to involve a stabilized carbanion intermediate. To provide reaction coordinate context for interpretation of the values of k_{cat}, k_{cat}/K_M, and kinetic isotope effects, we investigated the effect of solvent viscosity on k_{cat} and k_{cat}/K_M for the OMPDCs from *Methanothermobacter thermautotrophicus* (MtOMPDC) and *Saccharomyces cerevisiae* (ScOMPDC). For MtOMPDC, we used not only the natural OMP substrate but also a catalytically impaired mutant (D70N) and a more reactive substrate (FOMP); for ScOMPDC, we used OMP and FOMP. With MtOMPDC and OMP, k_{cat} is independent of solvent viscosity, indicating that decarboxylation is fully rate-determining; k_{cat}/K_M displays a fractional dependence of solvent viscosity, suggesting that both substrate binding and decarboxylation determine this kinetic constant. For ScOMPDC with OMP, we observed that both k_{cat} and k_{cat}/K_M are fractionally dependent on solvent viscosity, suggesting that the rates of substrate binding, decarboxylation, and product dissociation are similar. Consistent with these interpretations, for both enzymes with FOMP, the increases in the values of k_{cat} and k_{cat}/K_M are much less than expected based on the ability of the 5-fluoro substituent to stabilize the anionic intermediate, i.e., substrate binding and product dissociation mask the kinetic effects of stabilization of the intermediate by the substituent.

Orotidine 5'-monophosphate decarboxylase (OMPDC) that catalyzes the final step in the biosynthesis of pyrimidine nucleotides is an exceptionally proficient catalyst (Scheme 1) (2, 3). For the enzyme from *Saccharomyces cerevisiae* (ScOMPDC), the rate acceleration (k_{cat}/k_{non}) is 7.1×10^{16} ($k_{cat} = 20$ sec^{-1}; $k_{non} = 2.8 \times 10^{-16}$ sec^{-1}) and the proficiency [$(k_{cat}/K_M)/$

†This research was supported by NIH GM039754 (to J.P.R.) and GM065155 (to J.A.G.).

* To whom correspondence should be addressed: J.A.G.: Department of Biochemistry, University of Illinois, 600 S. Mathews Avenue, Urbana, IL 61801. Phone: (217) 244−7414. Fax: (217) 244−6538. E-mail: j-gerlt@uiuc.edu..

Cleland and coworkers did not report a value for k_{cat}/K_M for wild type ScOMPDC with OMP, so the value listed in the text is the one we determined; because our value for k_{cat} is 20 sec^{-1}, our value for k_{cat}/K_M should be a reliable measure of the catalytic efficiency of the enzyme used by Cleland. Our values for k_{cat} and k_{cat}/K_M for wild type ScOMPDC with FOMP are 130 sec^{-1} and 2.6×10^7 M^{-1} sec^{-1} (*vide infra*).

We have examined the effects of viscogens on the kinetic constants of mutants with substitutions for residues that are involved in the conformational changes that accompany ligand binding, e.g., the conserved Gln 215 in the active site loop and the conserved Ser 154 in a loop at the end of the fifth β-strand in ScOMPDC that "clamp" the liganded enzyme in a catalytically productive, closed conformation (1). These mutants display "complicated" effects, including increases, rather than decreases, in the values of the kinetic constants as viscosity is increased. We attribute these complexities to the details of the conformational changes that accompany ligand binding.

k_{non}] is 4.8×10^{22} M^{-1} ($k_{cat}/K_M = 1.3 \times 10^7$ M^{-1} sec^{-1}) (*vide infra*). These large values are explained by the very slow rate for the nonenzymatic reaction that results from the inability of the pyrimidine base to stabilize negative charge when decarboxylation occurs (4); this contrasts with pyridoxal phosphate-dependent amino acid decarboxylases, thiamin pyrophosphate-dependent α-ketoacid decarboxylases, and Schiff-base-dependent decarboxylases in which the negative charge is stabilized by an "electron sink." The structural strategy by which the rate acceleration and proficiency are accomplished remains both controversial and uncertain for the OMPDC-catalyzed reaction.

The sequences of homologous OMPDCs are surprisingly divergent, with four subfamilies recognizable in the databases; pairwise sequence identities between members of the different subfamilies can be <10% (J. A. Gerlt, P. C. Babbitt, and S. Brown, unpublished observations). However, the active site residues are strictly conserved, suggesting that these are fully responsible for achieving the rate acceleration and proficiency. Structures are available for at least one member from each subfamily (5-8); in the structures determined in the presence of intermediate analogs (azaUMP, 6-azaUMP, and BMP, barbiturate 5'-monophosphate) or the UMP product, C6/N6 of the pyrimidine base is proximal to a hydrogen-bonded Asp-Lys-Asp triad. The expectation is that this triad promotes decarboxylation, with the Lys delivering a solvent-derived hydrogen to C6 to form the UMP product.

The mechanism has been controversial; several have been proposed, including 1) preprotonation of O2 to form an electrostatically stabilized ylide intermediate by decarboxylation (9); 2) conjugate addition of a nucleophile to C5 followed by decarboxylation and elimination of the nucleophile (10); 3) a concerted S_E2 reaction in which decarboxylation and protonation of C6 occur simultaneously, avoiding the formation of a carbanionic intermediate (7,11); 4) and decarboxylation to form a vinyl anion intermediate stabilized by its proximity to the Lys of the hydrogen-bonded triad (12) and, possibly, by hydrogen bonding to O4 (13,14). The first two mechanisms are eliminated by the structures that reveal the absence of an acid proximal to O2 or a nucleophile to C5. The third mechanism is eliminated by two reports from our laboratories: 1) the solvent deuterium product isotope effect (PIE) for formation of the UMP product is 1.0 (no discrimination between protium and deuterium in delivery of a hydrogen to C6), arguing against a concerted mechanism in which decarboxylation and proton/deuteron-transfer occur in the same transition state (15); and 2) H6 of the UMP product undergoes exchange with solvent deuterium, requiring the formation of an intermediate with a sufficient lifetime for occasional rotation of the Lys in the hydrogen-bonded triad so that a solvent-derived hydrogen can be delivered to C6 (16). Thus, a mechanism involving an intermediate is secure (Scheme 1), although the structural strategy for stabilization of the intermediate is unknown.

Kinetic studies using mutant enzymes and/or substrate analogs can be expected to provide valuable details about the mechanism. However, interpretations of the values of both k_{cat} and k_{cat}/K_M as well as kinetic isotope effects (KIEs) require that the relative kinetic importance of the chemical steps (decarboxylation of OMP to yield the intermediate followed by its protonation to yield UMP) and physical steps (OMP binding and UMP release) be known. For example, Cleland and coworkers recently reported natural abundance [carboxy-^{13}C] KIEs on k_{cat}/K_M for ScOMPDC (12). For wild type, the values are 1.0255 ± 0.0005 (k_{cat}, 22 sec^{-1}; k_{cat}/K_M, 1.3×10^7 M^{-1} sec^{-1}) for OMP and 1.0106 ± 0.0001 (k_{cat}, 242 sec^{-1}; k_{cat}/K_M, 3.0×10^7 M^{-1} sec^{-1}) for the more reactive FOMP (the electronegative fluorine substituent stabilizes the intermediate by electron withdrawal; Scheme 2). With 2'-deoxyOMP and wild type ScOMPDC (k_{cat}, 0.15 sec^{-1}; k_{cat}/K_M, 2.8×10^4 M^{-1} sec^{-1}), the KIE increases to 1.0461 ± 0.0005; with OMP and the less active K59A mutant (k_{cat}, 0.52 sec^{-1}; k_{cat}/K_M, 7.1×10^2 M^{-1} sec^{-1}), the KIE further increases to 1.0543 ± 0.0002. The latter KIEs were interpreted as the

intrinsic value(s); the lesser values observed with wild type ScOMPDC using OMP and FOMP were interpreted in terms of an earlier transition state for FOMP than for OMP.

However, because these are KIEs on k_{cat}/K_M, mechanistic interpretations would be compromised if the energy barriers for substrate binding and the chemical steps were similar in magnitude. That the values of k_{cat}/K_M for OMP and FOMP are similar and approximate the diffusion-controlled limit suggests that decarboxylation is less rate-limiting for FOMP than for OMP. Also, Porter and Short reported a bimolecular rate constant of 6.2×10^7 M^{-1} sec^{-1} for the binding of OMP to ScOMPDC (17); the value of this rate constant suggests that substrate binding is partly rate determining and is reflected in the value of k_{cat}/K_m, 2×10^7 M^{-1} s^{-1} for the ScOMPDC-catalyzed reaction. Thus, the KIEs may not uniquely describe the transition states for decarboxylation (*vide infra*).

As a prelude to studies of mutants using both OMP and FOMP as substrates, we investigated the effects of both trehalose and sucrose on the values of k_{cat} and k_{cat}/K_M for both substrates using wild type ScOMPDC as well as the OMPDC from *Methanothermobacter thermautotrophicus* (formerly *Methanobacterium thermoautotrophicum;* MtOMPDC). Although their active site residues are conserved, ScOMPDC and MtOMPDC share ~20% sequence identity and differ in the length and structure of the active site loop that sequesters the substrate and intermediate from solvent. Changes in solvent viscosity can have significant effects on k_{cat} and k_{cat}/K_M for both enzymes, with the dependence on viscosity increasing with FOMP (physical steps more rate-determining) and decreasing when the values of the kinetic constants are decreased by an active site substitution (decarboxylation more rate-determining). These conclusions are important for deducing the structural basis for the 10^{17} rate acceleration, as illustrated by the studies described in the accompanying manuscript that examine the importance of substrate destabilization (18).

MATERIALS AND METHODS

Materials

Reagents were purchased from Sigma Aldrich at the highest purity available. Thrombin protease was purchased from GE Healthcare. All solutions were prepared with Millipore Ultrapure filtered water.

Syntheses of OMP and FOMP

The method described by van Vleet et al. was used with modifications to enzymatically synthesize both OMP and FOMP (12). A typical reaction (25 mL, 30 °C) for the synthesis of FOMP contained 11.4 mM 5'-phosphoribosyl 1'-pyrophosphate (PRPP, Sigma P8296; 1 eq), 13.7 mM 5-fluoroorotic acid (Sigma F5013, 1.2 eq), 47 U of orotate phosphoribosyltransferase (OPRTase) from *Salmonella typhimurium,* 130 U of yeast inorganic pyrophosphatase (Sigma I1643), 50 mM $MgCl_2$, and 100 mM Tris-HCl, pH 8.0. After 6 hrs, an additional 16 U of OPRTase and 90 U of pyrophosphatase were added, and the reaction was incubated overnight. The enzymes were removed using a 10 K NMWL membrane centrifugal filter (Millipore, 15 mL); the solution was diluted to 100 mL and loaded onto an anion exchange column (Dowex-1×8, 1.5 × 20 cm, Cl^-). The column was eluted with linear gradient (300 mL) of 0 to 0.8 M LiCl. Two peaks of UV absorbing material were detected. The first peak (eluting at 0.55 M LiCl) contained FOMP as determined by enzymatic assay with OMPDC. The product-containing fractions were pooled, the solvent was removed by rotary evaporation, and the residue was dissolved in water and lyophilized. The dry solid was washed with acetone:methanol (95:5) until it maintained a constant weight. The FOMP was dissolved in a small amount of water and precipitated by adding acetone:methanol (95:5) until the solution became cloudy. After storage overnight at 4 °C, the solid was recovered, dissolved in water,

and lyophilized. A total of 120 μmoles of FOMP was obtained (48%). ^{1}H NMR (D_2O, 500 MHz): δ5.15 (d, *J* = 3.2Hz, 1H), δ4.55 (q, *J* = 3.1 Hz, *J* = 6.9 Hz, 1H), δ4.19 (t, *J* = 6.9 Hz 1H), δ3.80 (m, 2H), δ3.71 (m, 1H).

The same procedure was used to prepare OMP except that orotic acid (Sigma O2750) was used instead of 5-fluoroorotic acid.

Orotate Phosphoribosyltransferase (OPRTase)

The gene encoding OPTRase was PCR-amplified from *Salmonella typhimurium* LT2 genomic DNA (ATCC 70072OD). The gene was ligated into the pET-17b (Novagen) vector using the *Nde*I/*Bam*HI restriction sites. The plasmid (pOPRTase) was maintained in *E. coli* XL1-Blue cells. For protein expression, the plasmid was transformed into *E. coli* BL21 (DE3) cells.

OPRTase was purified following the procedure of Bhatia *et al*. (19) with modifications. Six 6 mL cultures of E. *coli* BL21 (DE3) transformed with pOPRTase were grown overnight at 37 °C in LB containing 100 μg/mL ampicillin. The cultures were used to inoculate 6 × 2 L of LB broth containing 100 μg/mL ampicillin. The cultures were grown at 37 °C until the cell density reached an OD_{600} of 0.6. The cultures were then induced for protein production by addition of IPTG to a final concentration of 1 mM. After 5 hours, the cells were harvested by centrifugation and resuspended in 60 mL of buffer O (50 mM Tris-HCl, pH 8.0, 2 mM EDTA, and 2 mM β-mercaptoethanol) and lysed on ice by sonication using a 550 Sonic Dismembrator (Fisher Scientific) with 5 second pulses at 15 second intervals for a total of 10 minutes. The lysate was cleared by centrifugation at 15,000 rpm at 4 °C for 30 minutes. Four mL of 10% PEI (Sigma P3143, pH 8.0) was added to the lysate to remove nucleic acids; the precipitate was removed by centrifugation at 15,000 rpm at 4 °C for 30 minutes. An equal volume of 2 M $(NH_4)_2SO_4$ in buffer O was added to the lysate, and the solution was filtered through a 0.22 μm membrane (Millipore) to remove the debris. The solution was applied to a column of phenyl Sepharose (1.5 × 20 cm) pre-equilibrated with 1 M $(NH_4)_2SO_4$ in buffer O. The column was washed with 100 mL of 1 M $(NH_4)_2SO_4$ in buffer O, and the OPRTase was eluted with a linear gradient (800 mL) from 1 M to 0 M $(NH_4)_2SO_4$ in buffer O. Fractions containing OPRTase (identified by SDS-PAGE) were pooled and dialyzed at 4 °C three times against 2 L of Buffer O for a minimum of 3 hours. The OPRTase was further purified on a Resource Q column (1.5 × 10 cm; Pharmacia Biotech) pre-equilibrated with buffer O and eluted with a linear gradient (800 mL) from 0 to 0.5 M NaCl in Buffer O.

Fractions containing pure OPRTase were assayed in the direction of PRPP formation. The assay contained 0.1 mM OMP, 2 mM PP_i, 47 nM OPRTase, 20 mM potassium HEPES, pH 8.0, and 3 mM $MgCl_2$. The rate of the reaction was monitored by the change in absorbance at 303 nm [$\Delta\varepsilon = 2200\ M^{-1}\ cm^{-1}$ ($\varepsilon_{orotate} - \varepsilon_{OMP}$); $k_{cat} = 15\ sec^{-1}$]. OPRTase is stable at 4 °C for at least 3 months; freezing by dropwise addition to liquid N_2 and storage at −80 °C extends the storage time to one year. The activity was checked before each use.

Cloning, Expression, Site Directed Mutagenesis, and Purification

The gene encoding the OMPDC from *M. thermautotrophicus* ΔH (MtOMPDC) was amplified by PCR from genomic DNA (ATCC); *Nde*I and *Bam*HI digestion followed by ligation were used to clone the gene into pET-15b vector, resulting in the plasmid pMtODC-15b. The D70N mutant of MtOMPDC was constructed using the QuikChange II method [Stratagene;(18)]. DNA sequencing at the University of Illinois Core Sequencing Facility confirmed the expected sequences.

The vector pODC-C155S containing the gene encoding the C155S mutant of the OMPDC from *Saccharomyces cerevisiae* (ScOMPDC) (20) was a gift from Dr. Steven Short

(GlaxoSmithKline). The gene was excised using *Nde*I and *Bam*HI (Invitrogen) and ligated into the pET-15b vector encoding an N-terminal His_6-tag (Stratagene) using T4 DNA ligase (Fisher), resulting in the plasmid pScODC-15b. The D91N mutant of ScOMPDC was constructed using the QuikChange II method [Stratagene;(18)]. DNA sequencing at the University of Illinois Core Sequencing Facility confirmed the expected sequences.

Both wild type MtOMPDC and wild type ScOMPDC were purified from *E. coli* strain BL21 (DE3) (Promega). Transformed cells were grown in 4 L of LB containing 100 μg/mL ampicillin. For MtOMPDC, the cells were grown at 37 °C; when the cell density reached an OD_{600} of 0.6, IPTG was added at a final concentration of 0.5 mM. The cells were harvested after 18 hrs. For ScOMPDC, the cells were grown at 20 °C; after 24 hours, ScOMPDC was induced by the addition of IPTG to a final concentration of 0.5 mM. The cells were harvested after 48 hrs.

The same purification procedure was used for both enzymes. The cell pellet was resuspended in 100 mL of binding buffer (5 mM imidazole, 20 mM Tris-HCl, pH 7.9, 0.5 M NaCl) and sonicated on ice with 5 second pulses at 15 second intervals for a total of 36 minutes. The cell lysate was cleared by centrifugation, and the supernatant was loaded onto a Ni-Sepharose column (Pharmacia Biotech; 150 mL). The column was washed with 350 mL of binding buffer before 300 mL of a buffer containing 20 mM Tris-HCl, pH 7.9, 0.5 M NaCl, and 60 mM imidazole was used to remove contaminating proteins from the column. The N-terminal His_6-tagged OMPDC was eluted with a linear gradient (400 mL) from 60 mM to 1 M imidazole in binding buffer. Fractions containing OMPDC were identified by SDS-PAGE, pooled, and dialyzed at 5 °C against 3 × 4 L of 20 mM Tris-HCl, pH 7.9 for 3 hr intervals. Phosphate buffered saline was added along with 1 unit per mg of thrombin in order to remove the His_6-tag; the reaction was incubated for ~16 hrs at room temperature, with the progress monitored by SDS-PAGE. When the cleavage of the His_6-tag was completed, the reaction was dialyzed against 20 mM Tris-HCl, pH 7.9. The OMPDC was then applied to a Q-Sepharose High Performance column (Pharmacia Biotech; 50 mL) pre-equilibrated with 20 mM Tris-HCl, pH 7.9. After washing with 50 mL of 20 mM Tris-HCl, pH 7.9, the OMPDC was eluted with a linear gradient (500 mL) from 0 to 0.5 M NaCl in 20 mM Tris-HCl, pH 7.9. Fractions containing pure OMPDC were identified by SDS-PAGE and dialyzed at 5 °C against storage buffer. For MtOMPDC, the storage buffer was 20 mM HEPES, pH 7.5, 150 mM NaCl, and 3 mM DTT; for ScOMPDC, the storage buffer was 20 mM Tris-HCl, pH 7.9, 100 mM NaCl, and 20% glycerol. After concentration to ~ 25 mg/mL via ultrafiltration, the OMPDC was flash-frozen in liquid nitrogen as 25 μL pellets and stored at −80 °C.

The D70N mutant of MtOMPDC was purified by the same procedure, except the mutant was expressed in a *pyrF*$^{-}$ strain of *E. coli* generated using Wanner's method for chromosomal gene disruptions (21). Expression of the gene encoding the mutant in pET-15b was made possible using an chloramphenicol resistant auxillary plasmid, pTara, provided as a gift from Professor John Cronan, University of Illinois, which contains the T7 RNA polymerase under *araC* control. Growth was performed at 37 °C in LB containing 100 μg/mL ampicillin, 34 μg/mL chloroamphenicol, and 50 μg/mL kanamycin. Expression was induced by the addition of L-arabinose to a final concentration of 1 mM.

Viscogen Preparation and Viscosity Measurements

Viscogens were prepared as described in Hale et al. (22). Solutions of viscogens were prepared at twice the concentrations used in the enzymatic assays. For sucrose and trehalose, the final concentrations of the viscogens diluted into the reactions were 13.3, 15.6, 21.3, 26.7, 30, and 32%. Solutions of the macroviscogen Ficoll 400PM were prepared at final concentrations of 2.5, 5, and 10%. Relative viscosities were measured at 25 °C using an Ostwald viscometer (Fisher) and an analytical balance. The viscosities of each viscogen stock solution were

measured after dilution with an equal volume of 2X assay buffer (20 mM MOPS, pH 7.1 and 200 mM NaCl), η, relative to the 1X reaction buffer, η°. For sucrose, the relative viscosities were 1.41, 1.51, 1.87, 2.21, 2.60, and 2.74 for 13.3, 15.6, 21.3, 26.7, 30, and 32% sucrose, respectively. For trehalose, the relative viscosities were: 1.38, 1.52, 1.84, 2.24, 2.54, and 2.69 for 13.3, 15.6, 21.3, 26.7, 30, and 32% trehalose, respectively. For Ficoll 400PM, the relative viscosities were 1.53, 2.42, and 5.52 for 2.5, 5, and 10% Ficoll 400PM, respectively.

OMPDC Assays

All assays were performed at 25 °C and pH 7.1 (10 mM MOPS, containing 100 mM NaCl) (17) using a Cary UV/Vis spectrophotometer. For MtOMPDC, most assays contained 0.1 mg/mL BSA; however, determination of the values of k_{cat}/K_M for the wild type enzyme and OMP were performed in the absence of BSA to improve the signal-to-noise in the absorbance readings.

Concentrations of OMP and FOMP were measured spectrophotometrically: ε_{OMP} = 9430 M^{-1} cm^{-1} at 267 nm and ε_{FOMP} = 9895 M^{-1} cm^{-1} at 270 nm in 0.01 M HCl. A decrease in absorbance accompanies decarboxylation; assays were carried out at different wavelengths, depending on the initial substrate concentration. For decarboxylation of OMP, assays were conducted at 279 nm ($\Delta\varepsilon = -2400$) (21). For decarboxylation of FOMP, assays were conducted at 282 or 300 nm ($\Delta\varepsilon = -1378$ or -489 M^{-1} cm^{-1}, respectively), where 300 nm was used only for measuring the value of k_{cat} for wild type MtOMPDC.

The values of the K_Ms for both wild type MtOMPDC and ScOMPDC are ~ 1 μM. Therefore, because of limitations in the sensitivity of the spectrophotometric assay, initial velocity measurements as a function of substrate concentration could not be used to determine the values of K_M for the wild type enzymes (the kinetic constants for the D70N mutant of MtOMPDC were determined by measuring initial velocities as a function of substrate concentration). Instead, the values of k_{cat}/K_M were determined from the first-order decay of the absorbance when the concentration of remaining substrate was ≤ 20% of the estimated K_M value; the values of k_{cat} were determined in separate assays with substrate concentrations exceeding the estimated values of K_M by a factor ≥ 10. Because UMP is a competitive inhibitor for both MtOMPDC and ScOMPDC, low concentrations of substrate were used for measurement of the values of k_{cat}/K_M to minimize product inhibition that would increase the apparent value of K_M. Nonlinear, least squares curve fitting of each first order assay was performed with the program SigmaPlot using the first order equation

$$Abs = Abs_f + (Abs_i - Abs_s)\, e^{-kt}$$

where t is time, Abs is the absorbance at time t, Abs_f is the final absorbance Abs_i is the calculated initial absorbance, and k is the first order rate constant equal to V_{Max}/K_M.

RESULTS AND DISCUSSION

We are performing comparative studies of MtOMPDC and ScOMPDC with the expectation that, despite the divergence in sequence (the structure-based sequence identity is ~20%), the same structural strategy for catalysis is used by both enzymes. As a prelude to kinetic studies, we examined the effect of solvent viscosity on the kinetic constants for both OMP and FOMP to provide reaction coordinate context for interpretation of the values of the kinetic constants and isotope effects.

Experimental approach

We assume a simple kinetic mechanism (Scheme 3) that involves three sequential steps: 1) reversible OMP substrate binding (k_1 and k_{-1}), 2) irreversible decarboxylation and protonation to form bound UMP and CO_2 (k_2), and 3) reversible dissociation of UMP and CO_2 (k_3 and k_{-3}). In this mechanism, k_2 is independent of solvent viscosity (intramolecular within the active site), and those steps associated with substrate binding and product dissociation are assumed to be inversely proportional to the solvent viscosity (η_{rel}), e.g., $k_1 = k_1°/(\eta_{rel})$, with the superscript (°) noting the rate constant in the absence of viscogen. The rate constants associated with substrate binding (k_1 and k_{-1}) include encounter of the enzyme and substrate as well as conformational changes that juxtapose the substrate with the active site functional groups, including closure of an active site loop that sequesters substrate from solvent (18); the rate constant associated with product dissociation (k_3) includes conformational changes that include loop opening so that the product can dissociate from the enzyme.

The following relationships can be derived between the values of k_{cat} and k_{cat}/K_M and the various rate constants in the kinetic mechanism:

$$k_{cat} = \frac{k_2 k_3}{(k_2 + k_3)} \tag{1}$$

$$\frac{k_{cat}^{o}}{k_{cat}} = \frac{k_3^{o}}{(k_2 + k_3^{o})} + \frac{k_2}{(k_2 + k_3^{o})} \bullet \eta_{rel} \tag{2}$$

$$\text{slope} = \frac{k_{cat}^{o}}{k_3^{o}} \tag{3}$$

$$\frac{k_{cat}}{K_m} = \frac{k_1 k_2}{(k_{-1} + k_2)} \tag{4}$$

$$\frac{(k_{cat}/K_m)^{o}}{(k_{cat}/K_m)} = \frac{k_{-1}^{o}}{(k_{-1}^{o} + k_2)} + \frac{k_2}{(k_{-1}^{o} + k_2)} \bullet \eta_{rel} \tag{5}$$

$$\text{slope} = \frac{(k_{cat}/K_m)^{o}}{k_1^{o}} \tag{6}$$

Equations (1) and (4) are the steady-state expressions for k_{cat} and k_{cat}/K_M, respectively. Equations (2) and (5) describe the dependence of the values of k_{cat} and k_{cat}/K_M on solvent viscosity, respectively. Equations (3) and (6) relate the slopes of equations (2) and (5) with the values of $k_3°$ and $k_{cat}°$ and the values of $k_1°$ and $(k_{cat}/K_M)°$, respectively.

Studies of viscogen effects typically employ catalytically impaired mutants of residues that are involved directly in chemistry as essential controls, with the expectation that the kinetic constants for their reactions will be determined by the chemistry and, therefore, be independent

of solvent viscosity (Figure 1, panel A, red reaction coordinate) (23). An conceptually similar approach is to use a more reactive alternate substrate, with the expectation that if the rate of the chemical step is increased (*vide infra*), substrate binding and/or product dissociation steps will determine the values of kinetic constants, so that these will be inversely proportional to solvent viscosity (Figure 1, panel B, blue reaction coordinate). We have employed both approaches, the latter using FOMP, an alternate substrate expected to undergo more facile decarboxylation because of stabilization of the vinyl anion by the electron withdrawing substituent (18).

The studies reported in this manuscript were performed at pH 7.1, where the values of k_{cat} and k_{cat}/K_M using OMP as substrate are maximal for both MtOMPDC (4 sec^{-1} and 2.4×10^6 M^{-1} sec^{-1}, respectively) and ScOMPDC (20 sec^{-1} and 1.3×10^7 M^{-1} sec^{-1}, respectively) (17,18). Two “monomeric” microviscogens, sucrose and trehalose, and one polymeric macroviscogen, Ficoll 400PM, were used. Microviscogens influence both the measured viscosity and the diffusional behavior of solutes; macroviscogens influence the viscosity but have no effect on the diffusional behavior of solutes. Thus, Ficoll 400PM serves as a control to ensure that the viscosity effects produced by trehalose and sucrose are associated with diffusional processes involving 1) encounter of the enzyme and substrate (the contribution of k_1 to k_{cat}/K_M) and 2) separation of the enzyme and product (the contribution of k_3 to k_{cat}).

Viscogen Effects on MtOMPDC

D70N—Asp 70 in MtOMPDC has no apparent role in substrate binding, e.g., no hydrogen bonding interactions with intermediate analogs or the UMP product. We have implicated Asp 70 in destabilization of the substrate, with substitutions decreasing the values of k_{cat} and k_{cat}/K_M for both OMP (0.02 sec^{-1} and 5×10^3 M^{-1} sec^{-1}, respectively) and FOMP (4 sec^{-1} and 5×10^5 M^{-1} sec^{-1}, respectively) but having little influence on the rate of exchange of H6 of FUMP with solvent hydrogen (18). We selected the D70N mutant as a kinetically and structurally characterized control in which the substitution's role is restricted to decarboxylation, with the expectation that k_2 would be fully rate-determining.

Plots of the normalized values of both k_{cat} and k_{cat}/K_M for OMP as a function of relative solvent viscosity for D70N mutant of MtOMPDC are displayed in Figures 2A and 2B, respectively; analogous plots for FOMP are displayed in Figures 2C and 2D, respectively. The values of k_{cat} and k_{cat}/K_M as well as the slopes of the plots are tabulated in Table 1.

With both OMP and FOMP, the values of k_{cat} (0.02 sec^{-} and 4 sec^{-1}, respectively) are independent of solvent viscosity, indicating that for both substrates decarboxylation (k_2) is fully rate-determining ($k_2 << k_3°$) under saturating conditions. With both substrates, the values of k_{cat}/K_M also are independent of solvent viscosity, indicating that decarboxylation (k_2) is fully rate-determining under subsaturating conditions.

Therefore, as expected for an essential residue involved only in chemistry (Asp 70), decarboxylation (k_2) is fully rate-determining for both k_{cat} and k_{cat}/K_M (Figure 1, panel A). With this control, the viscosity dependence of the kinetic constants for wild type MtOMPDC can be evaluated.

Viscogen Effects on MtOMPDC

Wild Type—Plots of the normalized values of both $k_{cat}$and k_{cat}/K_M for OMP as a function of relative solvent viscosity for wild type MtOMPDC are displayed in Figures 3A and 3B, respectively; analogous plots for FOMP are displayed in Figures 3C and 3D, respectively. The values of k_{cat} and k_{cat}/K_M in the absence of viscogen as well as the slopes of the plots are tabulated in Table 1.

With OMP, for both microviscogens the value of k_{cat} (4 sec^{-1}) is independent of solvent viscosity, indicating that decarboxylation is fully rate-determining ($k_2 << k_3°$) under saturating conditions (Scheme 3). The value of k_{cat}/K_M is partially dependent on solvent viscosity (Figure 3B; slopes = 0.60 for sucrose and 0.59 for trehalose). From equation (6), the estimated value of $k_1°$ is 4.0×10^6 M^{-1} sec^{-}, 1.7-fold greater than the measured value of k_{cat}/K_M (2.4×10^6 M^{-1} sec^{-1}, Table 1). We conclude that under subsaturating conditions the value of k_{cat}/K_M is determined by both substrate binding ($k_1°$) and the chemical step (k_2).

With FOMP, for both microviscogens the value of k_{cat} is partially dependent on solvent viscosity ($k_{cat}° = 190$ sec^{-1}; slopes = 0.67 for sucrose and 0.59 for trehalose). From equation (3), the estimated value of $k_3°$ is ~ 300 sec^{-1}, consistent with the rates of decarboxylation and product release being comparable for the better substrate, as expected if the value of k_2 for FOMP is increased relative to that for OMP.

With FOMP, the value of k_{cat}/K_M is inversely proportional to solvent viscosity (Figure 3D; within error, the slopes for both microviscogens are unity). From equation (6), the value of $k_1°$ is approximately equal to the experimentally measured value of k_{cat}/K_M (4.8×10^6 M^{-1} sec^{-1}), i.e., k_{cat}/K_M is diffusion-controlled (by k_1) as a result of the increased value of k_2.

Therefore, for wild type MtOMPDC with OMP, we conclude that 1) k_{cat} measures the rate of decarboxylation of bound OMP ($k_2 << k_3°$) and 2) both substrate binding and decarboxylation contribute to the value of k_{cat}/K_M. That the values of k_{cat}/K_M for both OMP and FOMP are comparable in the absence of viscogens can be most simply explained if they contain significant contributions from substrate binding ($k_1°$), providing independent evidence for the conclusions obtained from the viscogen dependence.

Viscogen Effects on ScOMPDC

Wild Type—Plots of the normalized values of both k_{cat} and k_{cat}/K_M for OMP as a function of relative solvent viscosity for wild type ScOMPDC are displayed in Figures 4A and 4B, respectively; analogous plots for FOMP are displayed in Figures 4C and 4D, respectively. The values of k_{cat} and k_{cat}/K_M as well as the slopes of the plots are tabulated in Table 1.

With OMP, the value of k_{cat} is partially dependent on solvent viscosity ($k_{cat}° = 20$ sec^{-1}; slopes = 0.39 for sucrose and 0.31 for trehalose). From equation (3), the value of $k_3°$ is estimated ~60 sec^{-1}; this value modestly exceeds the measured value of k_{cat}, consistent with comparable rates of decarboxylation (k_2) and product release ($k_3°$) under saturating conditions.

The value of k_{cat}/K_M for OMP is also partially dependent on solvent viscosity (slopes = 0.37 for sucrose and 0.35 for trehalose). From equation (6), the value of k_1 is estimated as ~ 3.6×10^7 M^{-1} sec^{-1}, ~ 2.8-fold greater than the value of k_{cat}/K_M (1.3×10^7 M^{-1} sec^{-1}). We conclude that the value of k_{cat}/K_M is determined by both substrate binding ($k_1°$) and the chemical step (k_2).

With FOMP, the value of k_{cat} is inversely proportional to solvent viscosity for both microviscogens (slopes = 1.0), indicating that with the better substrate product dissociation is rate-determining ($k_2 >> k_3$). Compared to OMP, the value of k_{cat}/K_M for FOMP is more dependent on (slope = 0.65 for sucrose and 0.51 for trehalose), but not inversely proportional to, solvent viscosity, as would be expected if formation of the enzyme-substrate complex is rate-determining with the better substrate. From equation (6), the value of $k_1°$ is estimated as ~ 4.6×10^7 M^{-1} sec^{-1}, modestly greater than the experimentally measured value of k_{cat}/K_M (2.6×10^7 M^{-1} sec^{-1}).

Viscogen Effects on ScOMPDC

D91N?—We used the D70N mutant of MtOMPDC as a structurally and kinetically characterized control in which we were confident that the chemical step (k_2) would be rate-determining; the viscogen effects supported this expectation. However, we were unable to use the homologous D91N mutant as the analogous chemically impaired control for our studies of ScOMPDC. As described in the accompanying manuscript (18), the D91N substitution is virtually inactive with FOMP, with the structural data demonstrating that the 6-azaUMP competitive inhibitor binds to the unliganded conformation, with the active site loop open and the phosphate group, not the pyrimidine moiety, proximal to the active site hydrogen-bonded network that includes Asn 91.

Rate-Determining Conformational Changes (Active Site Loop Motion) in Substrate Binding and Product Release?

The values of k_{cat} for wild type MtOMPDC with OMP show a smaller viscosity dependence (slope = 0.0; Table 1) than the values for wild type ScOMPDC (slope ≈ 0.35); the partial dependence for ScOMPDC is consistent with Porter and Short's conclusion that product release is partially rate determining (17). The increase in the value of k_{cat} for wild type MtOMPDC with FOMP (48-fold) is greater than that observed for wild type ScOMPDC (6.5-fold), demonstrating stabilization of the carbanionic intermediate by the 5-fluoro substitution in the active sites of both enzymes. The partial viscosity dependence of k_{cat} for MtOMPDC with FOMP (slope ≈ 0.6) suggests that product release is partially rate determining, with the intrinsic effect of the 5-fluoro substituent larger than the observed 48-fold increase in the value of k_{cat} (recall the 200-fold effect of the 5-fluoro substituent for the D70N mutant). The inverse dependence of k_{cat} on viscosity for wild type ScOMPDC with FOMP (slope = 1.0) requires that product release be rate determining, i.e., $k_{cat} \approx k_3$. Thus, we conclude that the release of FUMP from MtOMPDC is faster than from ScOMPDC, perhaps because loop opening and closing is faster for the smaller active site loop in MtOMPDC (9 residues in MtOMPDC and 19 residues in ScOMPDC).

The value of k_{cat}/K_M for wild type MtOMPDC with OMP shows a partial viscosity dependence (slope ≈ 0.6), but the value of k_{cat}/K_M with FOMP shows an inverse viscosity dependence (slope = 0.9); this is the expected effect if the 5-fluoro substituent substantially increases the value of k_2 so that substrate binding is encountered-limited and fully rate-determining. In contrast, the values of k_{cat}/K_M for wild type ScOMPDC with OMP and FOMP both show partial viscosity dependence (slope ≈ 0.35 and 0.6, respectively), suggesting that a partially rate-limiting, viscosity independent, conformational change occurs after the initial encounter complex. That substrate binding, i.e., formation of the encounter complex and subsequent conformational change(s) to form the Michaelis complex, is fully rate-limiting for both MtOMPDC and ScOMPDC with FOMP is supported by the observation that the increased reactivity of FOMP is not associated with significant increases in the values of k_{cat}/K_M.

We suggest that the overall rate constant for formation of the Michaelis complex between FOMP and ScOMPDC limits the value of k_{cat}/K_M, but that the Michaelis complex forms in two kinetically distinct steps (Scheme 4). FOMP undergoes an encounter-limited reaction with a loop-opened conformation of ScOMPDC (E_o) to give an initial Michaelis complex (E_o•FOMP), which then closes with a partly rate-determining, viscosity-insensitive loop closure to form the catalytically active complex (E_c•FOMP). Following decarboxylation, the products are released by initial opening of the loop to generate E_o followed by product release.

The same two steps presumably are required for the MtOMPDC-catalyzed decarboxylation of FOMP. We suggest that the inverse viscosity dependence observed for this reaction reflects a larger rate constant for closing the smaller active site loop.

Conclusions

With wild type MtOMPDC and OMP, we conclude that 1) the value of k_{cat} is dominated by k_2, and 2) substrate binding contributes to the value of k_{cat}/K_M, with closure of the active site loop likely fast relative to encounter of the substrate and product. With wild type ScOMPDC and OMP, we conclude that 1) both decarboxylation and product dissociation contribute to the value of k_{cat} ($k_2 \sim k_3$), and 2) substrate binding, including reordering of the active site loop, contributes to the value of k_{cat}/K_M. These conclusions are consistent with the observations that 1) the values of k_{cat} for OMP and FOMP differ by "only" 7-fold with ScOMPDC, and 2) the values of k_{cat}/K_M are essentially the same for OMP and FOMP with both MtOMPDC and ScOMPDC.

An unequivocal explanation for the discrepancy between our observations (viscosity *dependent* values of k_{cat} and k_{cat}/K_M) and those reported by Wolfenden and coworkers (viscosity *independent* values of k_{cat} and k_{cat}/K_M) (24) is not possible. However, the values of K_M for ScOMPDC are known to be sensitive to ionic strength (17). We performed our assays in the recommended presence of 0.1 M NaCl; the experimental procedures provided by Wolfenden and coworkers did not indicate that ionic strength was maintained, so this may provide an explanation for the differing results.

Implications

Our conclusion that substrate binding contributes to the value of k_{cat}/K_M for wild type ScOMPDC for both OMP and FOMP contrasts with Cleland's interpretation regarding the structures of the transition states for their decarboxylation (12). "Full" intrinsic KIEs were measured for both 2'-deoxyOMP/wild type ScOMPDC (1.0461 ± 0.0005; k_{cat}/K_M, 2.8×10^4 M^{-1} sec^{-1}) and 2) OMP/K59A ScOMPDC (1.0543 ± 0.0002; k_{cat}/K_M, 7.1×10^2 M^{-1} sec^{-1}), with both substrate/enzyme pairs containing substitutions for contacts involved in substrate/intermediate binding, not chemistry. Lesser values for the KIEs were measured for OMP/wild type ScOMPDC (1.0255 ± 0.0005; k_{cat}/K_M, 1.3×10^7 M^{-1} sec^{-1}) and FOMP/wild type ScOMPDC (1.0106 ± 0.0001; k_{cat}/K_M, 3.0×10^7 M^{-1} sec^{-1}). The interpretation that the smaller value of the KIE for FOMP "suggests an earlier transition state" than for OMP may be incomplete, with a more complete explanation including that in both cases k_{cat}/K_M contains contributions from substrate binding, with these more important for FOMP than for OMP.

The accompanying manuscript describes kinetic studies of the D70N mutant of MtOMPDC that suggest that destabilization of the substrate contributes to the 10^{17} rate acceleration, with the quantitative interpretations therein based, in part, on the dissection of the relative importance of substrate binding, decarboxylation, and product dissociation accomplished in this manuscript (18).

Abbreviations

2'-deoxyOMP, 2-deoxyorotidine 5'-monophosphate
FOMP, 5-fluoroorotidine 5'-monophosphate
azaUMP, 6-azauridine 5'-monophosphate
BMP, 1-(5'-phospho-β-D-ribofuranosyl)barbituric acid
KIE, kinetic isotope effect
MtOMPDC, OMPDC from *Methanothermobacter thermautotrophicus*
OMP, orotidine 5'-monophosphate
OMPDC, orotidine 5'-monophosphate decarboxylase
OPRTase, orotate phosphoribosyltransferase
PRPP, 5'-phosphoribosyl 1'-pyrophosphate
ScOMPDC, OMPDC from *Saccharomyces cerevisiae*

UMP, uridine 5’-monophosphate
WT, wild type
η_{rel}, relative viscosity

REFERENCES

1. Barnett SA, Amyes TL, Wood BM, Gerlt JA, Richard JP. Dissecting the total transition state stabilization provided by amino acid side chains at orotidine 5'-monophosphate decarboxylase: a two-part substrate approach. Biochemistry 2008;47:7785–7787. [PubMed: 18598058]
2. Radzicka A, Wolfenden R. A proficient enzyme. Science 1995;267:90–93. [PubMed: 7809611]
3. Miller BG, Wolfenden R. Catalytic proficiency: the unusual case of OMP decarboxylase. Annu Rev Biochem 2002;71:847–885. [PubMed: 12045113]
4. Sievers A, Wolfenden R. Equilibrium of formation of the 6-carbanion of UMP, a potential intermediate in the action of OMP decarboxylase. J Am Chem Soc 2002;124:13986–13987. [PubMed: 12440884]
5. Miller BG, Hassell AM, Wolfenden R, Milburn MV, Short SA. Anatomy of a proficient enzyme: the structure of orotidine 5'- monophosphate decarboxylase in the presence and absence of a potential transition state analog. Proc Natl Acad Sci U S A 2000;97:2011–2016. [PubMed: 10681417]
6. Wu N, Mo Y, Gao J, Pai EF. Electrostatic stress in catalysis: structure and mechanism of the enzyme orotidine monophosphate decarboxylase. Proc Natl Acad Sci U S A 2000;97:2017–2022. [PubMed: 10681441]
7. Appleby TC, Kinsland C, Begley TP, Ealick SE. The crystal structure and mechanism of orotidine 5'-monophosphate decarboxylase. Proc Natl Acad Sci U S A 2000;97:2005–2010. [PubMed: 10681442]
8. Harris P, Navarro Poulsen JC, Jensen KF, Larsen S. Structural basis for the catalytic mechanism of a proficient enzyme: orotidine 5'-monophosphate decarboxylase. Biochemistry 2000;39:4217–4224. [PubMed: 10757968]
9. Rishavy MA, Cleland WW. Determination of the mechanism of orotidine 5'-monophosphate decarboxylase by isotope effects. Biochemistry 2000;39:4569–4574. [PubMed: 10769111]
10. Silverman RB, Gorziak MP. Model chemistry for a covalent mechanism of action of orotidine 5'-monophosphate decarboxylase. J Am Chem Soc 1982;104:6434–6439.
11. Begley TP, Appleby TC, Ealick SE. The structural basis for the remarkable catalytic proficiency of orotidine 5'-monophosphate decarboxylase. Curr Opin Struct Biol 2000;10:711–718. [PubMed: 11114509]
12. Van Vleet JL, Reinhardt LA, Miller BG, Sievers A, Cleland WW. Carbon isotope effect study on orotidine 5'-monophosphate decarboxylase: support for an anionic intermediate. Biochemistry 2008;47:798–803. [PubMed: 18081312]
13. Lee JK, Houk KN. A proficient enzyme revisited: the predicted mechanism for orotidine monophosphate decarboxylase. Science 1997;276:942–945. [PubMed: 9139656]
14. Houk KN, Lee JK, Tantillo DJ, Bahmanyar S, Hietbrink BN. Crystal structures of orotidine monophosphate decarboxylase: does the structure reveal the mechanism of nature's most proficient enzyme? Chembiochem 2001;2:113–118. [PubMed: 11828434]
15. Toth K, Amyes TL, Wood BM, Chan K, Gerlt JA, Richard JP. Product deuterium isotope effect for orotidine 5'-monophosphate decarboxylase: evidence for the existence of a short-lived carbanion intermediate. J Am Chem Soc 2007;129:12946–12947. [PubMed: 17918849]
16. Amyes TL, Wood BM, Chan K, Gerlt JA, Richard JP. Formation and stability of a vinyl carbanion at the active site of orotidine 5'-monophosphate decarboxylase: pKa of the C-6 proton of enzyme-bound UMP. J Am Chem Soc 2008;130:1574–1575. [PubMed: 18186641]
17. Porter DJ, Short SA. Yeast orotidine-5'-phosphate decarboxylase: steady-state and pre-steady- state analysis of the kinetic mechanism of substrate decarboxylation. Biochemistry 2000;39:11788–11800. [PubMed: 10995247]
18. Chan KK, Wood BM, Fedorov AA, Fedorov EV, Imker HJ, Amyes TL, Richard JP, Almo SC, Gerlt JA. Mechanism of the Orotidine 5’ Monophosphate Decarboxylase Catalyzed Reaction: Evidence for Substrate Destabilization. Biochemistry 2009;48submitted
19. Bhatia MB, Vinitsky A, Grubmeyer C. Kinetic mechanism of orotate phosphoribosyltransferase from Salmonella typhimurium. Biochemistry 1990;29:10480–10487. [PubMed: 2271660]

20. Sievers A, Wolfenden R. The effective molarity of the substrate phosphoryl group in the transition state for yeast OMP decarboxylase. Bioorg Chem 2005;33:45–52. [PubMed: 15668182]

21. Datsenko KA, Wanner BL. One-step inactivation of chromosomal genes in *Escherichia coli* K-12 using PCR products. Proc Natl Acad Sci U S A 2000;97:6640–6645. [PubMed: 10829079]

22. Hale SP, Poole LB, Gerlt JA. Mechanism of the reaction catalyzed by staphylococcal nuclease: identification of the rate-determining step. Biochemistry 1993;32:7479–7487. [PubMed: 8338846]

23. Blacklow SC, Raines RT, Lim WA, Zamore PD, Knowles JR. Triosephosphate isomerase catalysis is diffusion controlled. . Biochemistry 1988;27:1158–1165. [PubMed: 3365378]

24. Miller BG, Snider MJ, Short SA, Wolfenden R. Contribution of enzyme-phosphoribosyl contacts to catalysis by orotidine 5'-phosphate decarboxylase [In Process Citation]. Biochemistry 2000;39:8113–8118. [PubMed: 10889016]

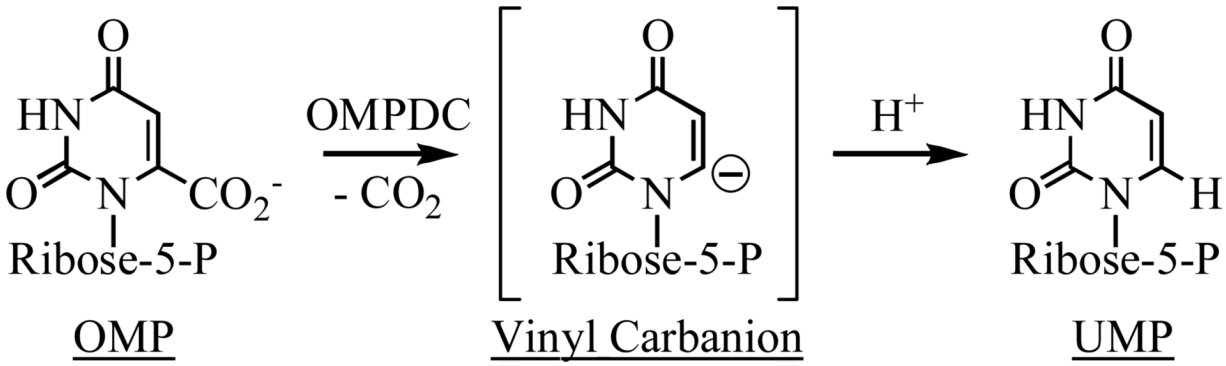

Scheme 1.

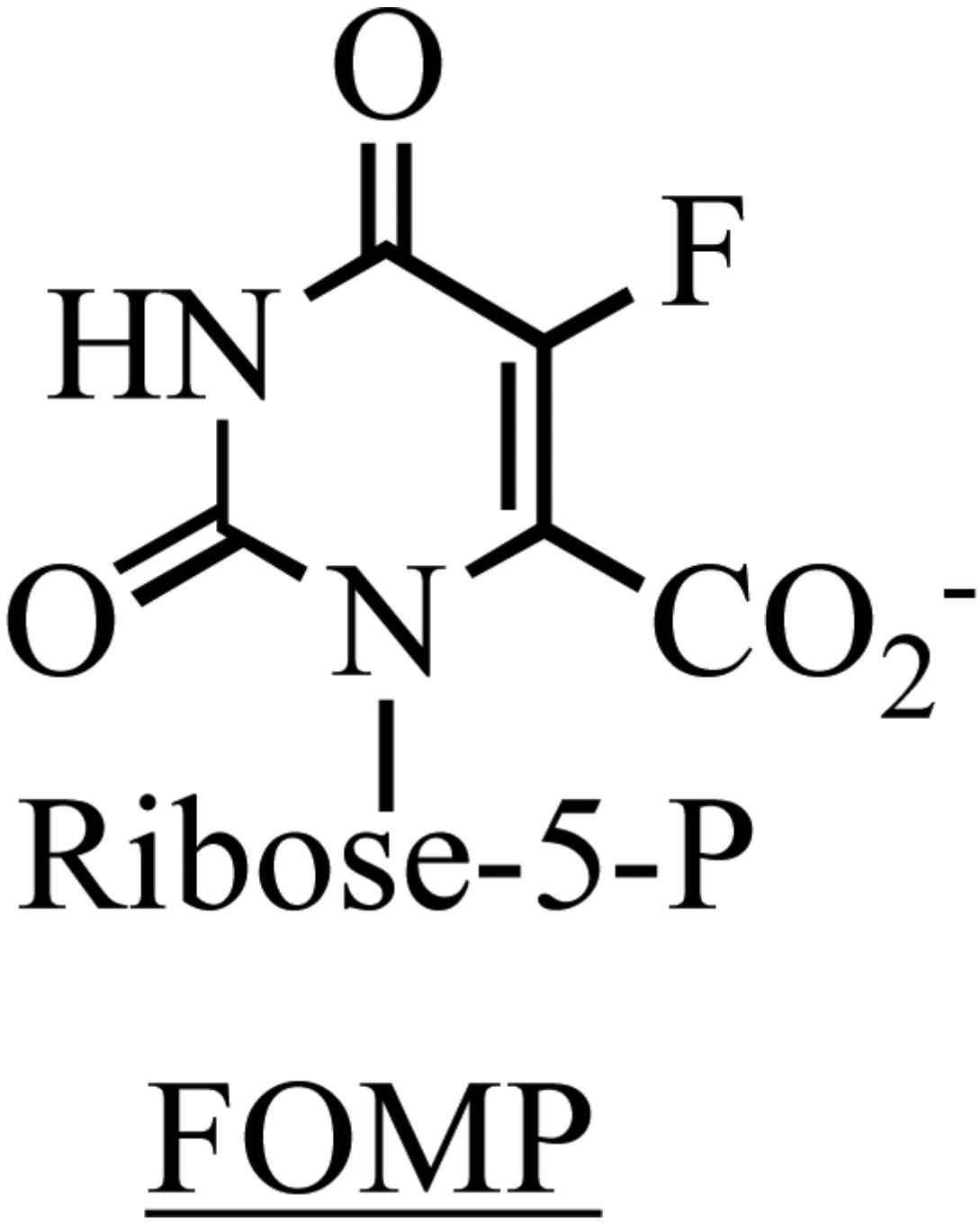

FOMP

Scheme 2.

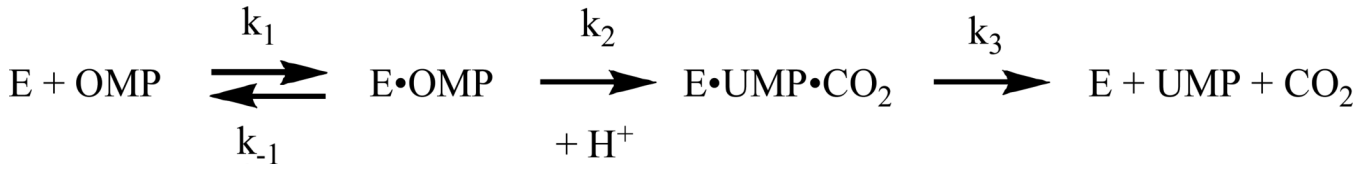

Scheme 3.

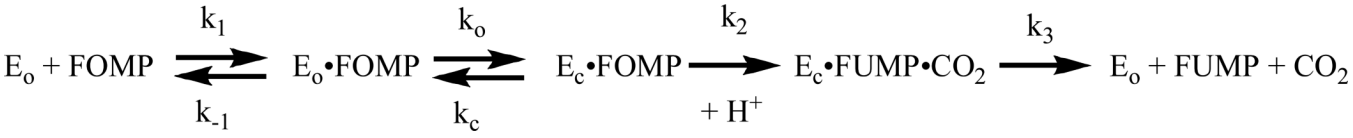

Scheme 4.

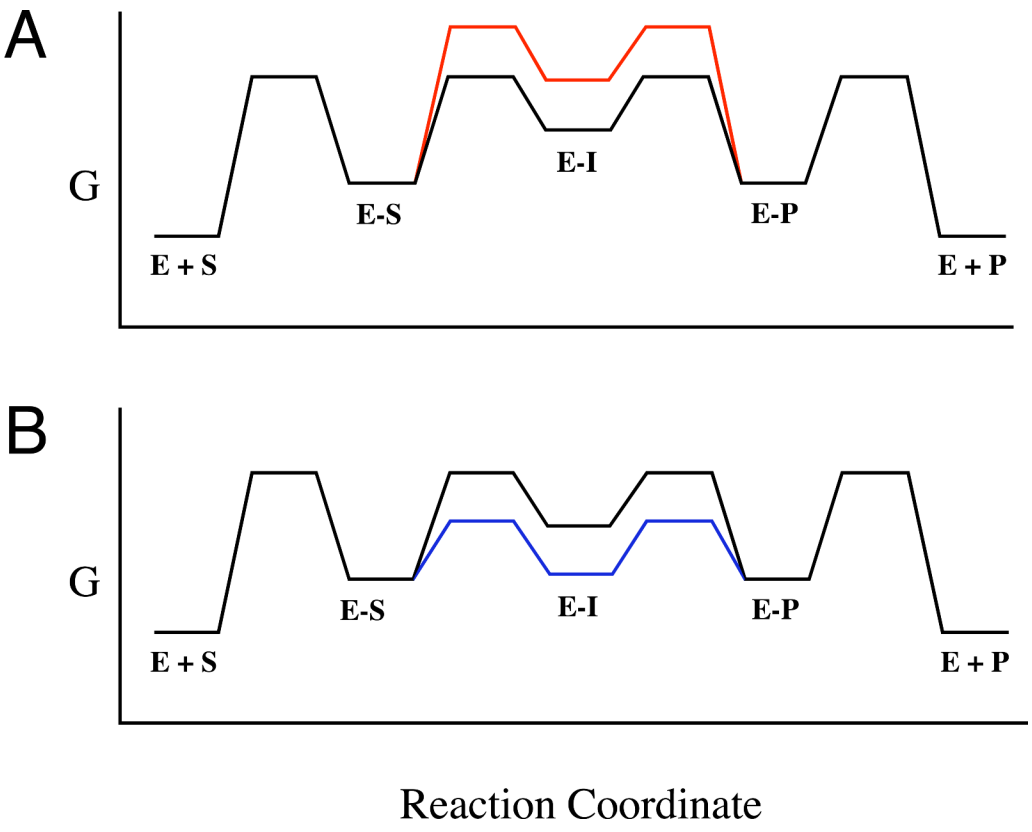

Figure 1.

Panel A, qualitative reaction coordinates for the OMPDC-catalyzed reaction in which 1) the transition states for substrate binding, decarboxylation/protonation, and product dissociation are equivalent in energy (black) and 2) the energies of the transition states for decarboxylation/protonation are increased by substitution for an active site residue, e.g., the D70N mutant of MtOMPDC (red). Panel B, qualitative reaction coordinates for decarboxylation in which 1) the transition states for substrate binding, decarboxylation/protonation, and product dissociation are equivalent in energy (black) and 2) the energies of the transition states for decarboxylation/protonation are decreased with a better substrate, e.g., FOMP (blue). These reaction coordinates are for [S] << K_M because the E-S complex is at a higher energy than E + S.

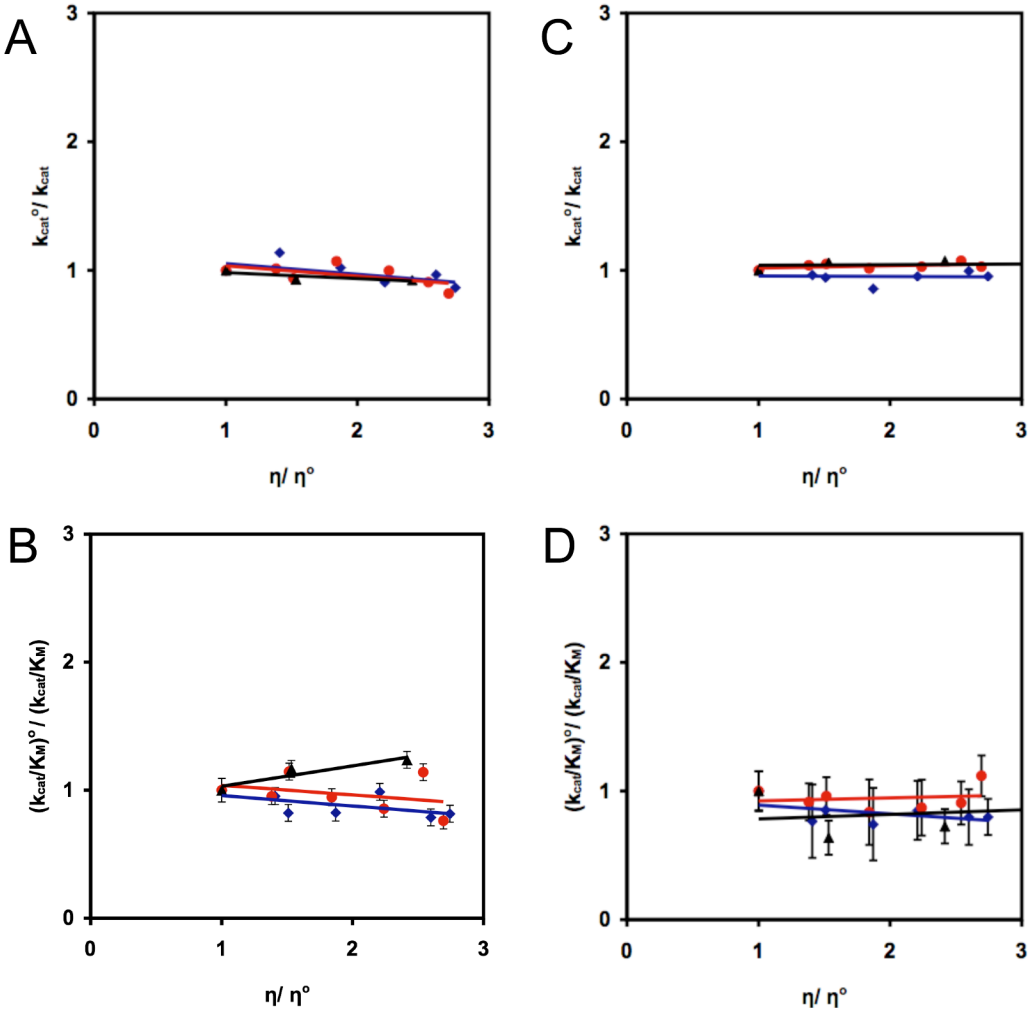

Figure 2.

Plots of the normalized values of k_{cat} and k_{cat}/K_M for decarboxylation of OMP and FOMP by the D70N mutant of MtOMPDC as a function of relative solvent viscosity; the data for sucrose are shown in blue and those for trehalose are shown in red. Panel A, k_{cat} for OMP. Panel B, k_{cat}/K_M for OMP. Panel C, k_{cat} for FOMP. Panel D, k_{cat}/K_M for FOMP.

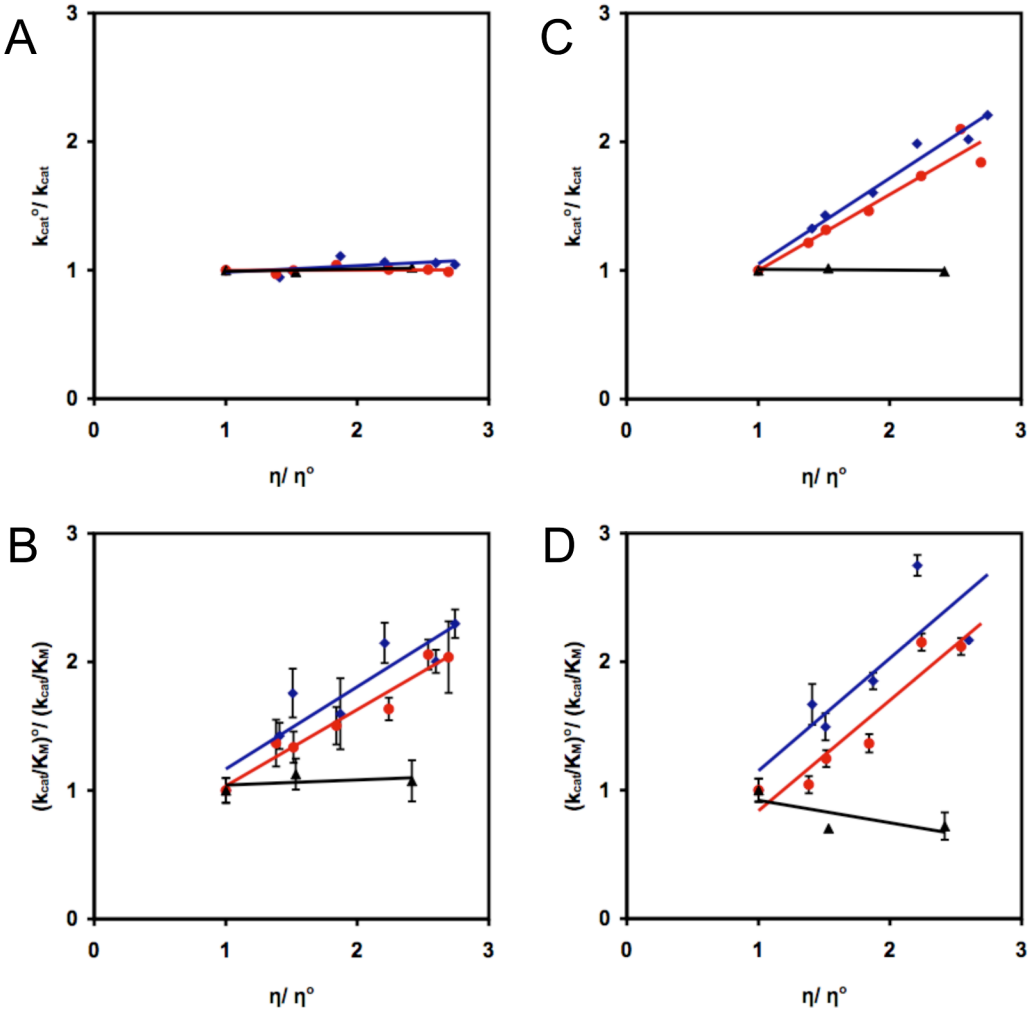

Figure 3.

Plots of the normalized values of k_{cat} and k_{cat}/K_M for decarboxylation of OMP and FOMP by wild type MtOMPDC as a function of relative solvent viscosity; the data for sucrose are shown in blue and those for trehalose are shown in red. Panel A, k_{cat} for OMP. Panel B, k_{cat} for FOMP. Panel C, k_{cat}/K_M for FOMP.

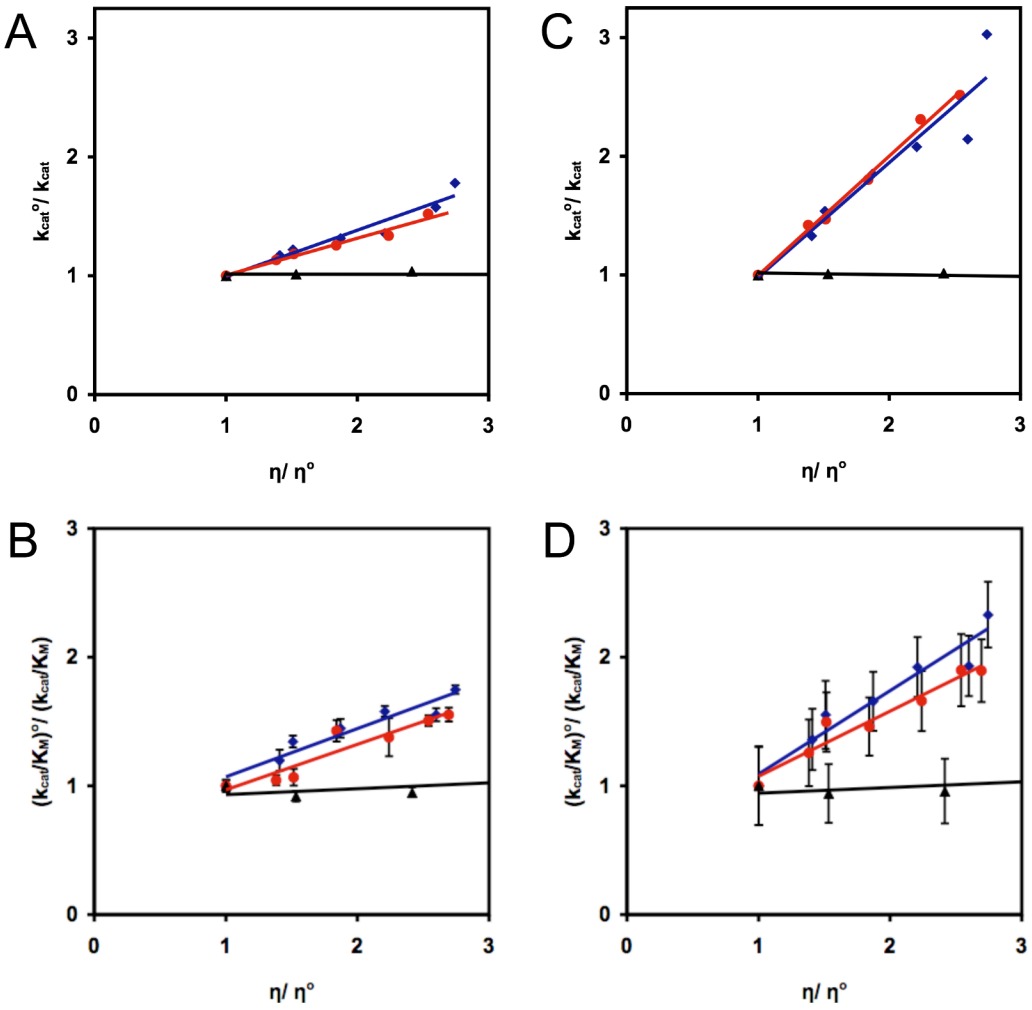

Figure 4.

Plots of the normalized values of k_{cat} and k_{cat}/K_M for decarboxylation of OMP and FOMP by wild type ScOMPDC as a function of relative solvent viscosity; the data for sucrose are shown in blue and those for trehalose are shown in red. Panel A, k_{cat} for OMP. Panel B, k_{cat}/K_M for OMP. Panel C, k_{cat} for FOMP. Panel D, k_{cat}/K_M for FOMP.

Table 1

Viscosity dependence of the values of k_{cat} and k_{cat}/K_M for MtOMPDC and ScOMPDC[a]

	OMP						FOMP					
	k_{cat} (s^{-1})	Slope[b] k_{cat}/k_3^o	k_3^o (s^{-1})	k_{cat}/K_M ($M^{-1}s^{-1}$)	Slope[c] $(k_{cat}/K_M)/k_1^o$	k_1^o ($M^{-1}s^{-1}$)	k_{cat} (s^{-1})	Slope[b] k_{cat}/k_3^o	k_3^o (s^{-1})	k_{cat}/K_M / $M^{-1}s^{-1}$	Slope[c] $(k_{cat}/K_M)/k_1^o$	k_1^o ($M^{-1}s^{-1}$)
D70N	0.02			5×10^3			4			5×10^5		
sucrose		0.02 ± 0.04	-[d]		−0.08 ± 0.05	-[d]		−0.01 ± 0.03	-[d]		−0.07 ± 0.05	-[d]
trehalose		−0.01 ± 0.02	-[d]		−0.08 ± 0.09	-[d]		0.02 ± 0.02	-[d]		0.02 ± 0.07	-[d]
ficoll		0.09 ± 0.07	-[d]		0.16 ± 0.06	-[d]		0.01 ± 0.01	-[d]		0.04 ± 0.06	-[d]
MtOMPDC	4			2.4×10^6			190			4.8×10^6		
sucrose		0.05 ± 0.03	-[d]		0.60 ± 0.10	4.0×10^6		0.67 ± 0.05	280		0.9 ± 0.3	5.3×10^6
trehalose		0.00 ± 0.01	-[d]		0.59 ± 0.06	4.1×10^6		0.59 ± 0.07	320		0.9 ± 0.1	5.3×10^6
ficoll		0.02 ± 0.02	-[d]		0.04 ± 0.08	-[d]		−0.01 ± 0.02	-[d]		−0.2 ± 0.2	-[d]
ScOMPDC	20			1.3×10^7			130			2.6×10^7		
sucrose		0.39 ± 0.05	50		0.37 ± 0.05	3.3×10^7		1.0 ± 0.2	130		0.65 ± 0.08	4.0×10^7
trehalose		0.31 ± 0.03	60		0.35 ± 0.06	3.3×10^7		1.01 ± 0.04	130		0.51 ± 0.06	5.1×10^7
ficoll		0.00 ± 0.01	-[d]		0.05 ± 0.02	-[d]		0.01 ± 0.01	-[d]		0.04 ± 0.02	-[d]

[a] All assays were conducted at 25 °C in 100 mM NaCl and 10 mM MOPS, pH 7.1 (I = 0.105 M).

[b] $\Delta(k_{cat})$norm/ $\Delta(\eta_{rel})$

[c] $\Delta(k_{cat}/K_M)$norm/ $\Delta(\eta_{rel})$

[d] When the kinetic constants are independent of solvent viscosity, equations (2) and (4) cannot be used to estimate values of k_3^o and k_1^o, respectively.